SUPPLEMENTAL METHODS AND FIGURES

Supplemental Methods

Isolation and use of primary bone marrow-derived mouse macrophages. Mouse bone marrow cells were isolated from 1-2 femurs of 8-week old female C57BL/6 mice largely as described (1). The cells were cultured at ~10^6 cells/ml in complete media [RPMI 1640, 10% HI FBS (Invitrogen), 1% penicillin/streptomycin] and 100 ng/ml mouse r-MCSF (Peprotech); ~6 ml of the cell suspension was added to 25-cm^2 rectangular, canted ultra-low attachment flasks (Corning). The medium was refreshed after 3 days. On the fifth day, the cells were dislodged by gentle scraping, counted, and plated at ~10^6 cells/ml in 1 ml fresh MCSF-supplemented complete media with 50 μg/mL oxLDL in 24-well ultralow attachment plates (Corning), with 3-4 replicates seeded per condition in each of two independent experiments. On day 6, the cells were incubated with estradiol for 48 h, and the conditioned media and cell pellets were collected and analyzed, as described for human macrophages (see Methods).

Isolation and use of primary mouse vascular SMCs. Primary mouse SMCs were isolated from 8-12 weeks old female WT mice. SMCs were prepared by explant culture as described previously (2). SMCs were maintained in growth medium (1:1 Dulbecco's modified Eagle's medium (DMEM)/Ham's F-12 supplemented with 2 mM L-glutamine) with 10% FBS and used between passages two to five. Near confluent monolayers were serum-starved with 1 mg/ml heat-inactivated fatty acid-free BSA for 48 hours, and then stimulated with 20 ng/ml PDGF and 1% FBS in the presence of selected concentrations of estradiol for 24 h.

Analysis of atherosclerosis. To identify overall lesion burden, the isolated aorta was rinsed with 50% isopropanol for 2 min, incubated in 0.67% Oil-Red-O for 15 min, and washed with 10% isopropanol for 2 min. Results were imaged with a Nikon SMZ800 stereoscope and captured on a Nikon DXM1200F digital camera. The area of each lesion was measured with Image Pro Plus

software (Version 3.0.1; Media Cybernetics, Inc., Silver Spring, Maryland) and expressed as percentage of atherosclerotic area relative to total area of the aorta.

To analyze aortic roots, isolated hearts were embedded in optimal cutting temperature medium (OCT). Frozen sections of the aortic root (10 μm) were fixed in 3.7% formaldehyde and washed three times in PBS. The sections were then blocked with 3% BSA in PBS for 15-30 min at room temperature before immunostaining. Some sections were stained with anti-CD68 (ab53444, Abcam; diluted 200:1 in PBS, 1% BSA) and FITC-conjugated anti-α-SMA monoclonal antibody (F3777, Sigma-Aldrich; diluted 200:1 in PBS, 1% BSA) followed by Alexa Fluor 594-conjugated goat anti-rat IgG (A11007, Invitrogen; diluted 250:1 in PBS). The percentage of CD68 or SMA-positive lesion was determined as in (3). Briefly, lesions were delineated using the polygon tool in ImageJ, and raw integrated densities and areas were obtained. Raw Integrated Density/Area was calculated and corrected for background by subtracting the mean Raw Integrated Density/Area from randomly selected regions lacking tissue. The results are recorded as percentage of total aortic root area.

Some sections were co-stained with anti-CD68 and anti-MMP12 to determine the amount of MMP12 in male vs female CD68-positive lesions. Detection of CD68 was performed as above, and detection of MMP12 was performed with anti-MMP12 (ab52897, Abcam; diluted 50:1 in PBS, 1% BSA). Secondary antibodies were Alexa Fluor 594-conjugated goat anti-rabbit IgG (A11012: Invitrogen) and Alexa Fluor 488-conjugated donkey anti-rat IgG (A21208; Invitrogen). Aortic root lesions co-stained with anti-CD68 and anti-MMP12 were analyzed in Fiji. The freehand tool was used to trace and measure the outer and inner borders of the anti-CD68 staining, and these traced borders were transferred digitally to the MMP12 image. The integrated density and area of the MMP12 signal within the CD68+ region was then determined in Fiji for each tracing. Subtraction of the MMP12 "inner" integrated density/area" measurement from the corresponding "outer" measurement yielded the MMP12 signal intensity within the CD68+ lesion.

In situ elastase assay. Elastase activity was quantified by in situ zymography of aortic root sections of LDLR-/-;MMP12$^{+/+}$ and LDLR-/-;MMP12$^{-/-}$ mice, largely as described (4, 5). Frozen cryostat OCT sections (10 μm) were placed in a dark humidified chamber and incubated overnight at room temperature with 40 μg/ml fluorescein (FAM)-conjugated elastin (85113, AnaSpec) that had been dissolved in Novex zymogram developing buffer (LC2671, Invitrogen). The samples were washed three times with PBS and imaged at 40 x magnification. Elastase activity, detected as green fluorescence, was quantified using Image J. The region of elastase activity for each region was outlined using the polygon tool to obtain raw integrated density (RawIntDen) and sample area. A mean background signal (RawIntDen/area) for each region was determined from three randomly selected regions without tissue. The net RawIntDen/area (total signal minus background) was then calculated for each section and normalized to the mean elastase activity of the LDLR-/-;MMP12$^{+/+}$ samples. The net signals from three near-adjacent sections were calculated, averaged, and graphed.

Collagen analysis. For collagen-I staining, aortic root lesion sections were washed in PBS, blocked in PBS, 3% BSA and incubated overnight at 4^{o}C with anti-collagen-I (1310-10, Southern Biotech; diluted 250:1 in PBS) followed by washing and a 2-h incubation with TRITC-AffiniPure F(ab)2 fragment rabbit anti-goat IgG (305-026-003, Jackson ImmunoResearch Laboratories). Trichome staining used standard procedures.

Reverse transcription quantitative PCR (RT-qPCR). For the mRNA analysis of mouse aortas, 1-2 mm sections of thoracic aortas near the diaphragm were pooled and stored in RNAlater (Qiagen) prior to isolation of RNA with RNeasy (Qiagen). For the human and mouse macrophages, total RNA was isolated using the RNAqueous micro kit (ThermoFisher) as per manufacturer's instructions. DNAse treatment was conducted on thawed RNA using the DNAse 1 Amplification Grade Kit (ThermoFisher). For human and mouse SMCs, cells were collected in

1 ml of TriZol (ThermoFisher) and RNA isolation performed according to the manufacturer's instructions. Reverse transcription reactions contained 50-100 ng of total RNA, except for experiments with human SMCs, which used 250-500 ng. Ten-fifteen percent of the cDNA was subjected to qPCR (6) with the following primer-probe sets from Applied Biosystems: mouse MMP-2 (Mm00439496), mouse MMP-9 (Mm00442991), mouse MMP12 (Mm00500554), human MMP12 (Hs00899662), and 18S RNA. The primer-probe set for 18S rRNA has been described (6). Results were normalized to 18S rRNA and plotted as ddCt. For experiments with human macrophages, the qPCR analysis used SYBR green reagents (Thermo Fisher Scientific) and 100 ng cDNA per reaction. The SYBR green primers were custom-designed and synthesized by Thermo Fisher Scientific and used at a final concentration of 150 nM. The primer sequences were: TGTAAGCAGGAACTTGGACTCG (human MMP12 forward primer), CCTGTCTCCTGCTTCAAAACC (human MMP12 reverse primer), AAGGTGAAGGTCGGAGTCAAC (human GAPDH forward primer) and GGGGTCATTGATGGCAACAATA (human GAPDH reverse primer). Results were calculated using ddCt and normalized to GAPDH mRNA.

Atomic Force Microscopy (AFM). Arterial stiffness (elastic moduli) was measured with a BioScope AFM (Bruker) in force mode as previously described (3, 7). Briefly, the AFM was performed using a silicon nitride probe (0.06 N/m cantilever) with a spherical tip (1-μm diameter SiO2 particle). We indented on the lumenal face of freshly isolated aortas, longitudinally opened. To focus on ECM mechanics and minimize the confounding effect of lipid deposits, we avoided probing regions with visible lesions. Twenty-five force curves from five different locations in each aorta were collected, and four different aortas were tested per condition. To compute the elastic modulus, the first 600 nm of tip deflection from the horizontal was fitted with the Hertz model for a cone.

Supplemental References

1. Su S, Su S, Liu J. Isolation of mouse bone marrow-derived monocytes. *Protoc. Exch.* [published online ahead of print: September 14, 2015]; doi:10.1038/protex.2015.081

2. Cuff CAA et al. The adhesion receptor CD44 promotes atherosclerosis by mediating inflammatory cell recruitment and vascular cell activation. *J Clin Invest* 2001;108(7):1031–1040.

3. Kothapalli D et al. Cardiovascular Protection by ApoE and ApoE-HDL Linked to Suppression of ECM Gene Expression and Arterial Stiffening. *Cell Rep.* 2012;2(5):1259–1271.

4. Liu S-L et al. Matrix metalloproteinase-12 is an essential mediator of acute and chronic arterial stiffening. *Sci. Rep.* 2015;5. doi:10.1038/srep17189

5. Johnson JL et al. A Selective Matrix Metalloproteinase-12 Inhibitor Retards Atherosclerotic Plaque Development in Apolipoprotein E–Knockout Mice. *Arterioscler. Thromb. Vasc. Biol.* 2011;31(3):528–535.

6. Klein EAA, Yung Y, Castagnino P, Kothapalli D, Assoian RKK. Cell adhesion, cellular tension, and cell cycle control. *Methods Enzym.* 2007;426:155–175.

7. Bae YH, Liu S-L, Byfield FJ, Janmey PA, Assoian RK. Measuring the stiffness of Ex vivo mouse aortas using atomic force microscopy. *J. Vis. Exp.* 2016;2016(116). doi:10.3791/54630

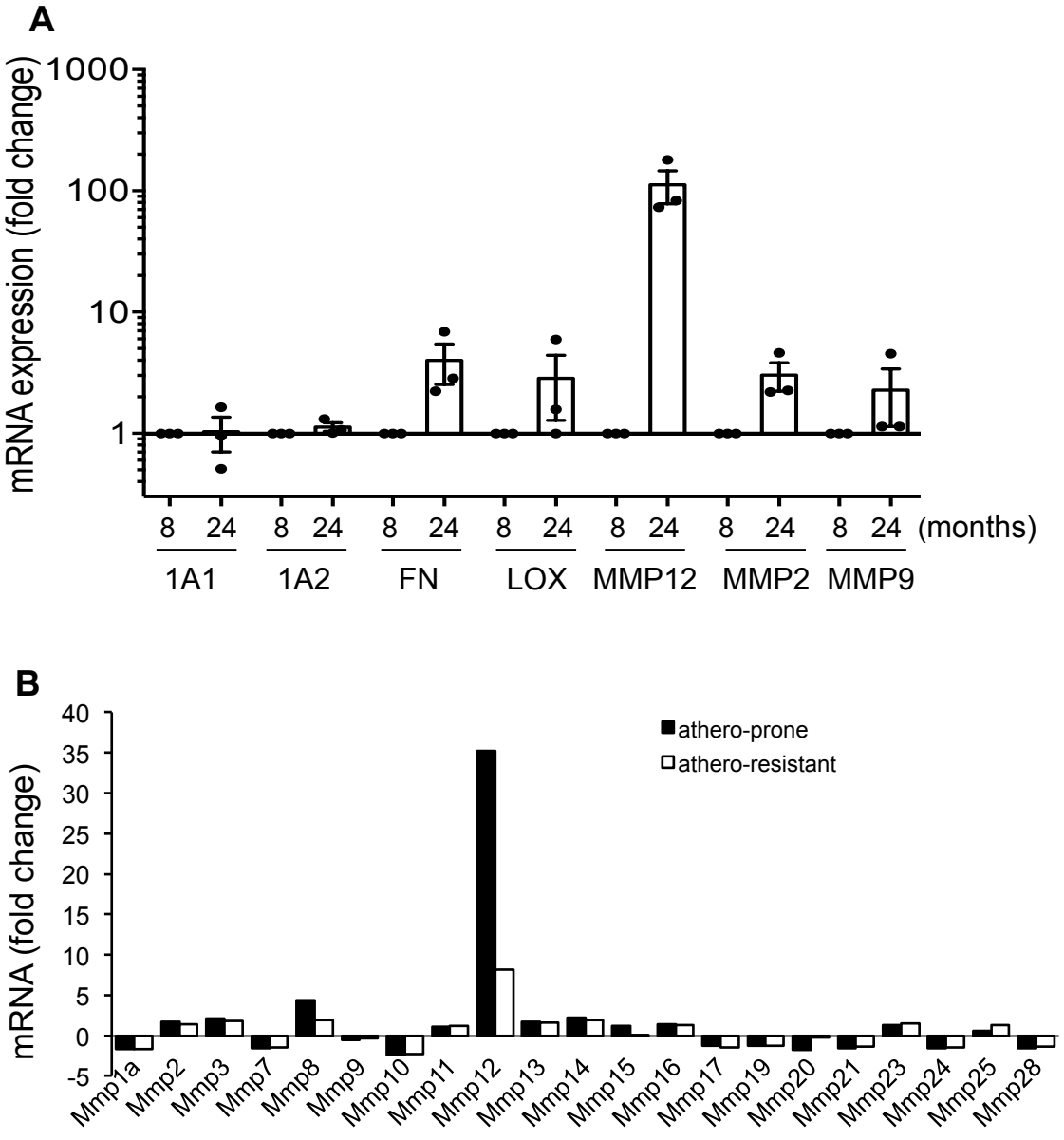

Figure S1. Preferential induction of MMP12 mRNA in atherosclerosis. (A) RT-qPCR analysis of freshly isolated aortas from male LDLR$^{-/-}$ mice after high-fat diet from 8-24 weeks. Results show mean ± SD and are normalized to the abundance of each transcript (Col1a1, 1A1; Col1a2, 1A2; fibronectin, FN; Lysyl oxidase, LOX; and MMPs 12, 2 and 9) in the 8-week sample; n=3 with each independent experiment pooling aortas from 4 mice. **(B)** Differential expression of the MMPs in 4-mo athero-prone and athero-resistant regions of apoE-null vs. WT mouse arteries as determined by microarray analysis, largely as described (3), of GEO Dataset GSE13865.

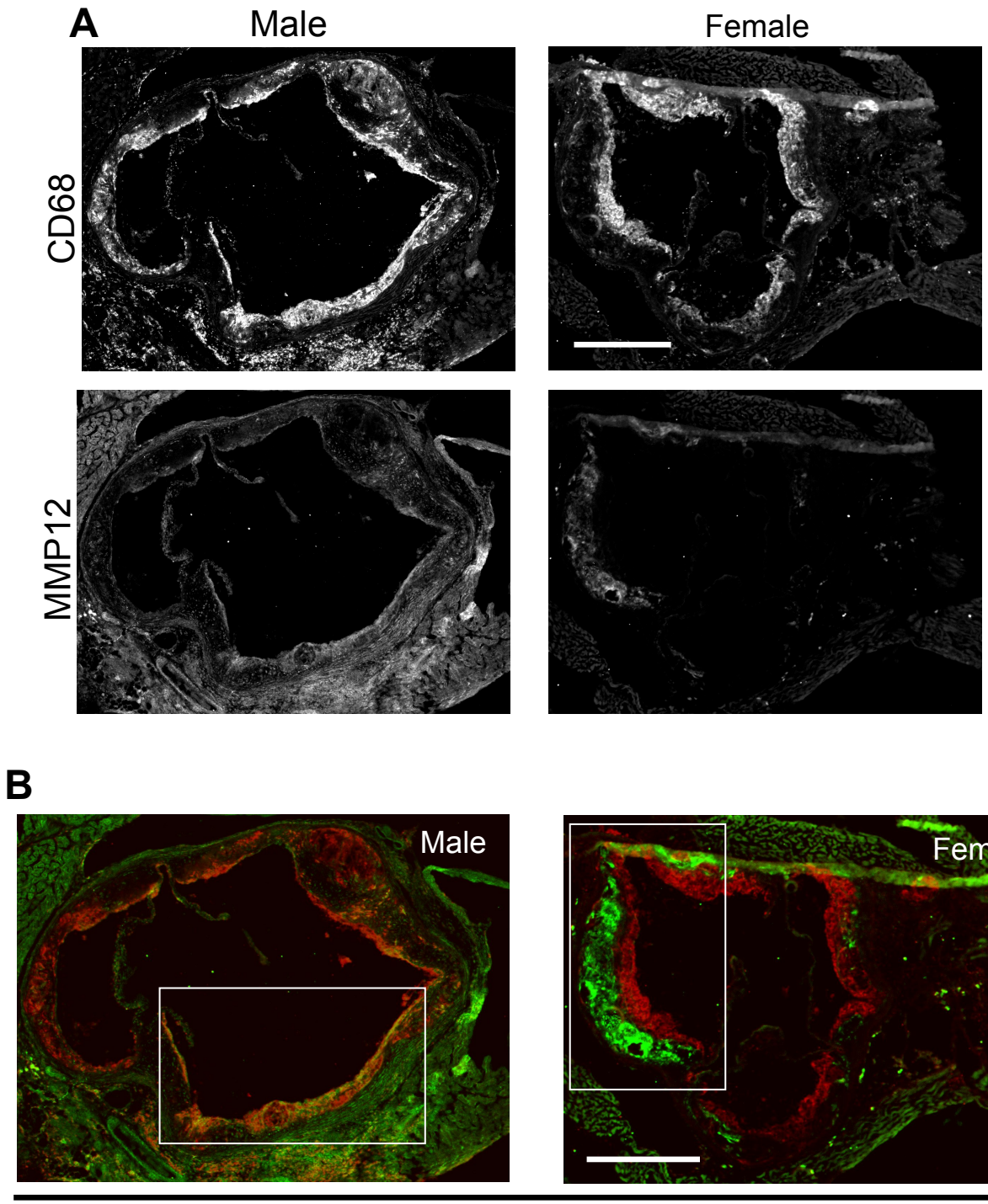

Figure S2. Primary images for CD68 and MMP12 immunostaining. Unmerged **(A)** and merged **(B)** Unmerged images of aortic root section stained for CD68 and MMP12 and used in Fig. 2C. The white boxes in the bottom panels outline the regions of interest shown in Fig. 2C. Scale bars = 500 μm.

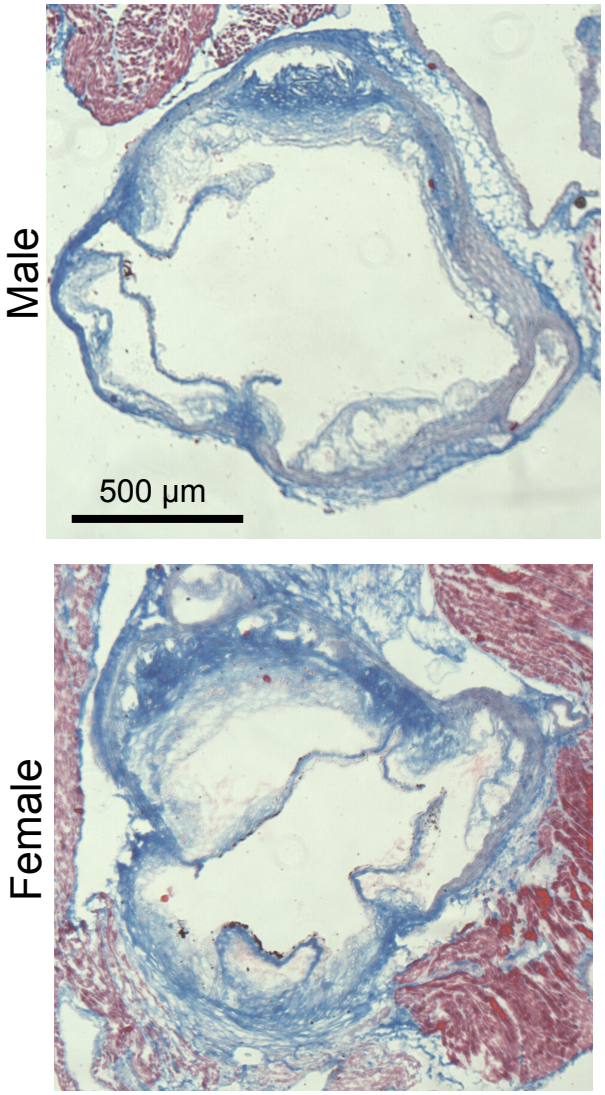

Figure. S3. Representative trichrome staining. Aortic roots from male (n=6) and female (n=6) LDLR$^{-/-}$ mice fed a high fat diet from 2-6 months were sectioned and stained with trichome.

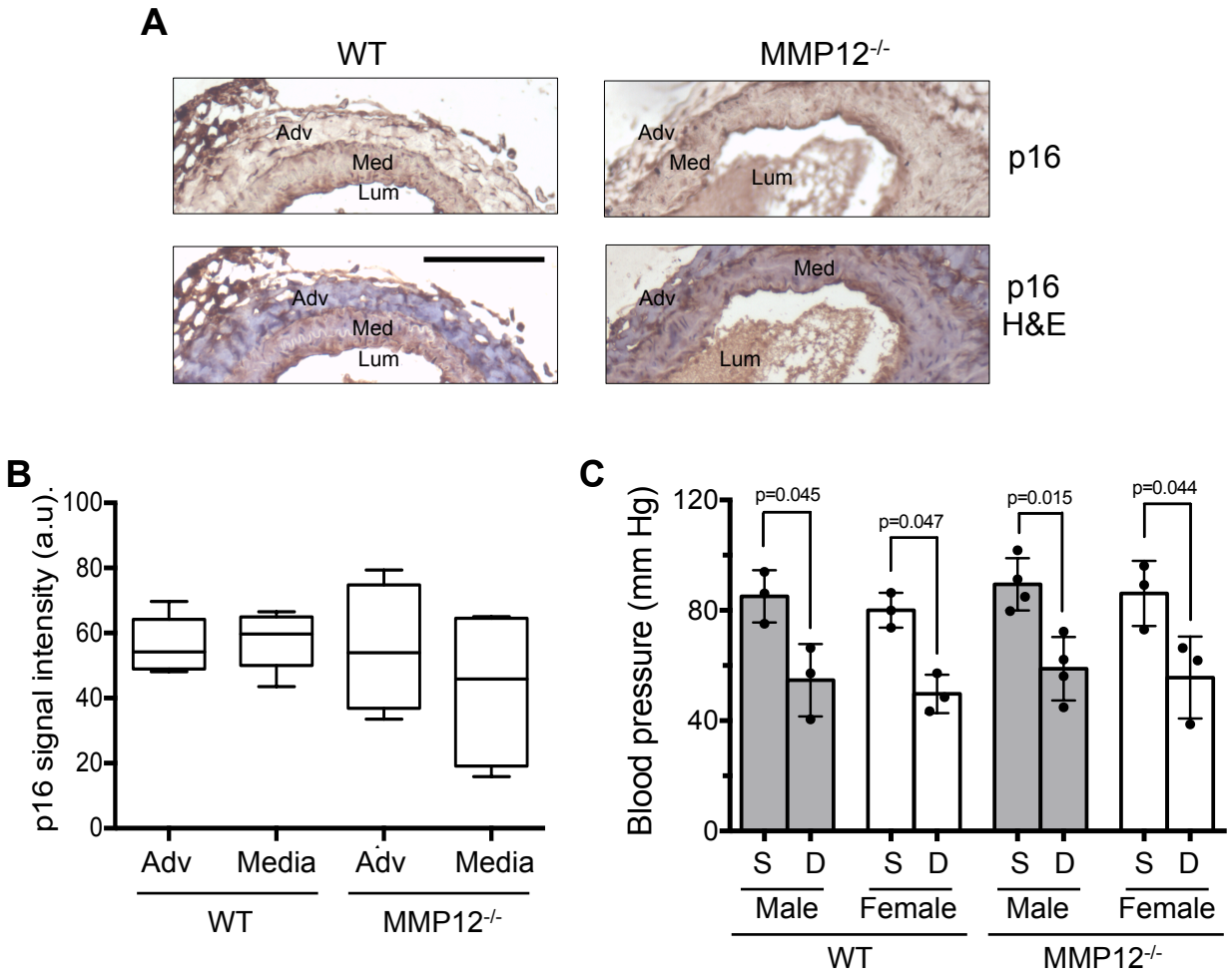

Figure S4. Similar arterial p16INK4a expression and blood pressure in WT and MMP12-null mice. (A-B) Carotid arteries isolated from 2-year old male WT (n=5) and MMP12$^{-/-}$ (n=4) mice. The arteries were fixed in Prefer, embedded in paraffin, sectioned, and stained with anti-p16INK4a (Proteintech; #10883-1-AP), biotinylated goat anti-rabbit IgG (1:1500 Vector labs; #BA-1000), and ABC-Elite solution (Vector Labs; PK-6100). Background signal was determined using normal rabbit IgG. DAB was used for color development. Panel A shows representative images: Adv (adventitial layer), Med (medial layer), Lum (lumen). Panel B shows quantification of all samples in Fiji after conversion to 8-bit, inverted images and correction for background signal. The data in panel B are shown as a box and whisker plot with Tukey whiskers; the horizontal lines of boxes represent the 25th percentile, the median, and the 75% percentile. **(C)** Left ventricular systolic (S) and diastolic (D) blood pressure of 6-month old male and female WT and MMP12$^{-/-}$ mice (n=3 per condition) was determined by invasive hemodynamics and show mean ± SD. Statistical significance between gender, MMP12 status, and systolic vs. diastolic pressures was tested by ANOVA. Only systolic and diastolic blood pressures within each condition were statistically different.

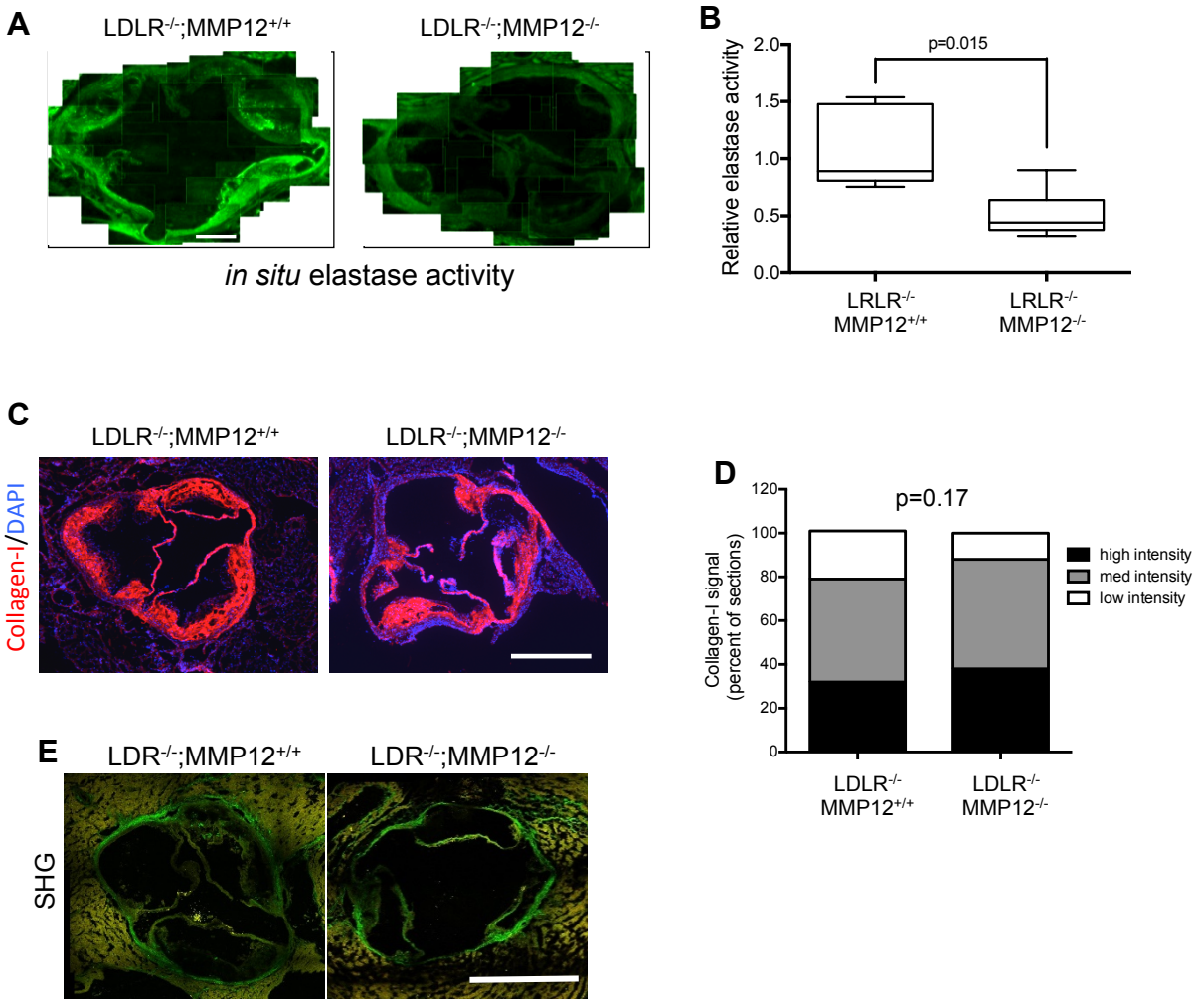

Figure S5. Elastase activity, but not collagen-I abundance or structure, are affected by MMP12 deletion in LDLR$^{-/-}$ mice. (A) Representative images of in situ elastase activity (green) in aortic root sections of male LDLR$^{-/-}$ and LDLR$^{-/-}$;MMP12$^{-/-}$ on high fat diet from 2-6 months. The figure shows a composite of images taken at 40 x magnification; scale bar = 200 μm. **(B)** Quantification of results in A expressed as percentage of aortic root area; n = 6 per genotype. The data in panel B are shown as a box and whisker plot with Tukey whiskers; horizontal lines of the boxes represent the 25th percentile, the median, and the 75% percentile. **(C)** Representative images of aortic root lesions isolated from male LDLR$^{-/-}$ and MMP12$^{-/-}$;LDLR$^{-/-}$ mice on a high-fat diet from 2-6 months analyzed by immunofluorescence microscopy for total collagen-I (red) and DAPI-stained nuclei (blue). **(D)** Blinded quantification of collagen-I immunostained sections (n=10 mice, with 3 near-adjacent sections/mouse, per genotype); p-value determined by chi-square test. **(E)** Representative images of aortic root sections from LDLR$^{-/-}$ (n=6) and MMP12$^{-/-}$;LDLR$^{-/-}$ (n=3) mice prepared as in C and analyzed by SHG micrographs. Scale bars = 500 μm.

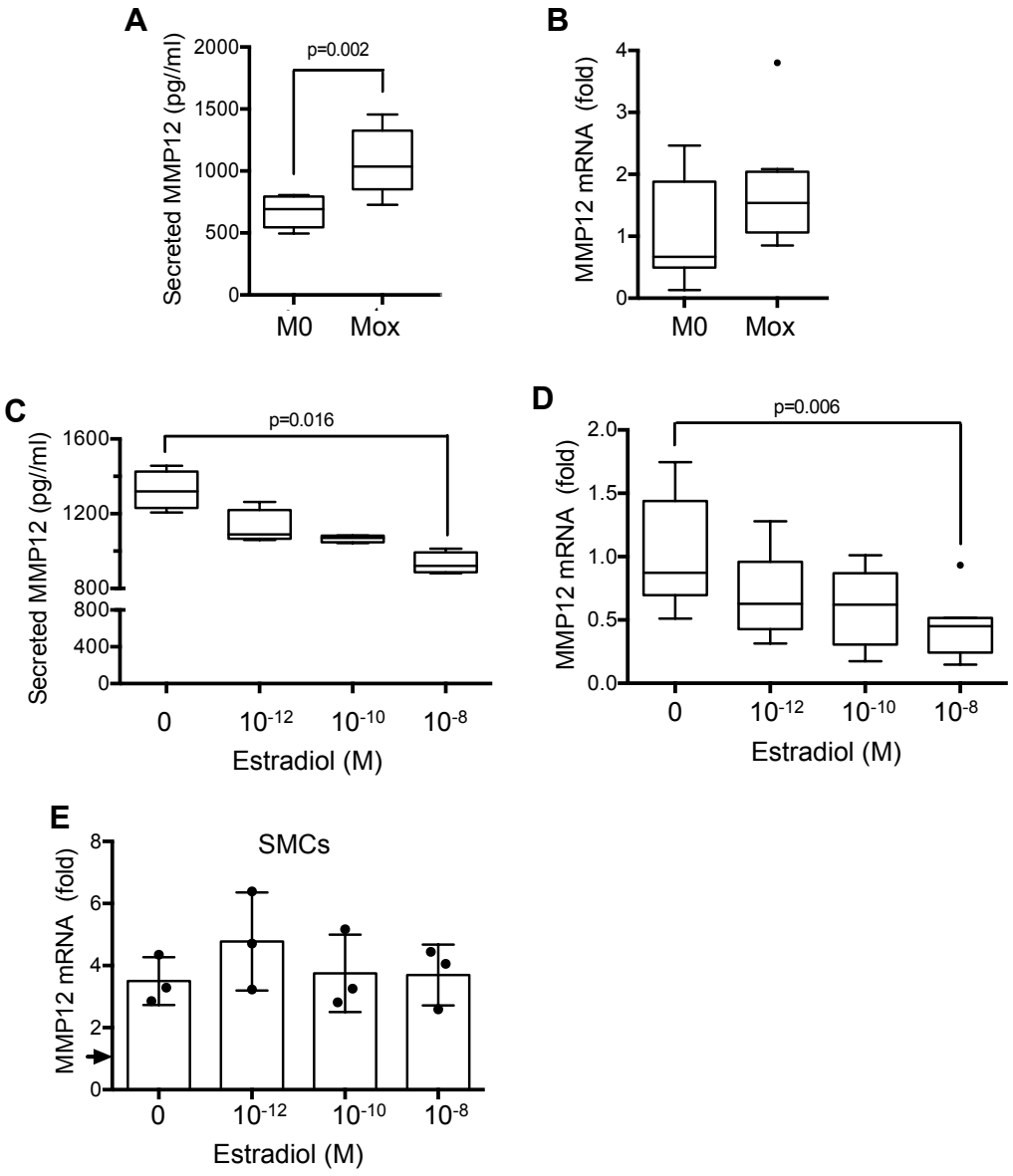

Figure S6. Estrogen inhibits MMP12 gene expression and secreted MMP12 in murine Mox macrophages. (A-D) The experimental approach outlined in Fig. 4 for human cells was applied to freshly isolated female bone marrow-derived monocytes from 8-week old C57BL/6 mice (n=8). Statistical significance in A-B and C-D was determined using Mann-Whitney tests and ANOVAs, respectively. The data in panels A-D are shown as box and whisker plots with Tukey whiskers; the horizontal lines of boxes represent the 25th percentile, the median, and the 75% percentile. **(E)** Near confluent primary explant aortic SMCs isolated from 8-12 week female C57BL/6 mice were serum-starved for 2 days, pre-incubated for 30 min with 0-10^{-8} M estradiol, activated with 20 ng/ml PDGF and 1% FBS, and incubated for 24 h. MMP12 mRNA levels were measured by RT-qPCR and plotted relative to 18S rRNA; n=3. Results show mean ± SD and are plotted relative to the serum-starved cells lacking estradiol (arrow). Statistical significance was determined by ANOVA.

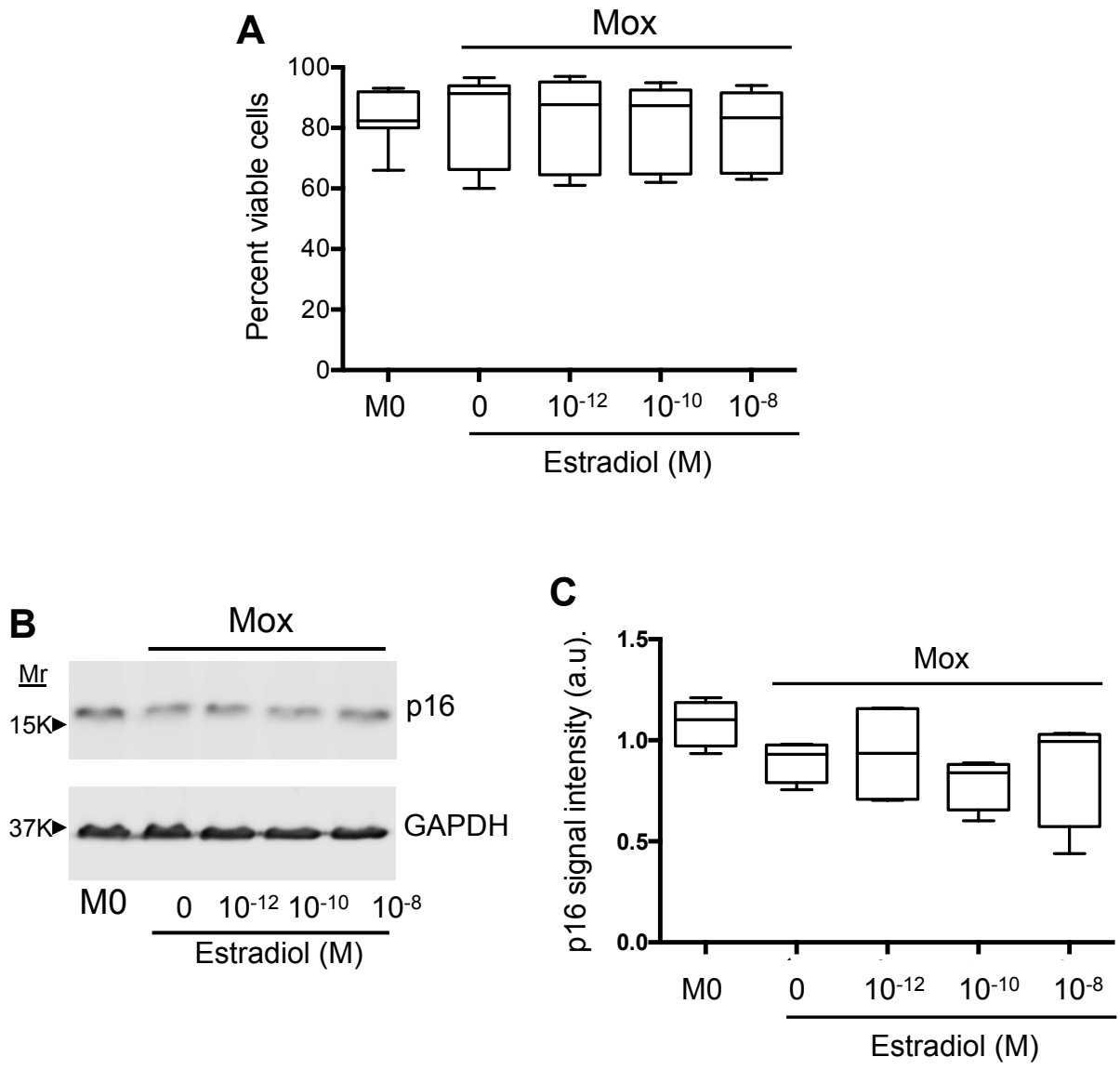

Figure S7. Macrophage viability is unaffected by oxLDL or estradiol. Female human peripheral blood-derived monocytes were differentiated into M0 macrophages, treated with oxLDL, and exposed to selected concentrations of estradiol (E2) as described in Methods. **(A)** Cells were collected from each replicate after the 48 h incubation with E2, and viability was determined using Trypan Blue; n=11-12. **(B)** Cell pellets lysed in SDS-sample buffer with β-mercaptoethanol were fractionated on 15% SDS-gels. Fractionated protein were, transferred nitrocellulose and blotted with anti-$p16^{INK4A}$ (Proteintech # 10883-1-AP**)** and anti-GAPDH (Invitrogen MA5-15738). **(C)** Signal intensities of p16 and GAPDH were determined from gels scanned in Fiji. p16/GAPDH ratio, calculated for each sample, was defined as p16 signal intensity; n=4. Data in A and C are shown as a box and whisker plots with Tukey whiskers; the horizontal lines of boxes represent the 25th percentile, the median, and the 75% percentile. Statistical significance was tested using ANOVA.